Original Article
18F-DOPA PET with and without MRI fusion, a receiver operator characteristics comparison

Aaron F Struck[1,3], Lance T Hall[1], Joanna E Kusmirek[1], Catherine L Gallagher[2,3], John M Floberg[4], Christine J Jaskowiak[1], Scott B Perlman[1]

[1]Department of Radiology University of Wisconsin School of Medicine and Public Health, Madison, WI, USA; [2]William S. Middleton Memorial VA, Madison, WI, USA; [3]Department of Neurology University of Wisconsin School of Medicine and Public Health, Madison, WI, USA; [4]Department of Medical Physics, University of Wisconsin – Madison, Madison, WI, USA

Abstract: This study is a retrospective analysis of the diagnostic accuracy of FDOPA PET with MRI fusion to FDOPA PET without MRI fusion. Clinical FDOPA PET scans obtained between 2000 and 2008 at the University of Wisconsin Hospital and Clinics were assessed using measures derived from regions of interest (ROI) generated with fused MRI (fused group) and again with ROIs derived solely from PET data (non-fused groups). The ROIs were used to calculate ratios (Striatum/Occipital cortex, Striatum/Cerebellum) pertinent to Parkinson's disease (PD) pathology. The clinical records were assessed for demographic data, follow-up length, and diagnosis. Receiver Operator Characteristics with area under the curve (AUC) measures were calculated and compared using confidence intervals and hypothesis testing. 27 patients had FDOPA PET with median clinical follow-up of 4 years. Of these, 17 patients had FDOPA PET with a fusible MR image. Seven of the 27 had a non-PD movement disorder. AUCs for the ratio measures ranged from 0.97-1.0 (fused), 0.73-0.83 (non-fused), and 0.63-0.82 (matched non-fused). The fused images had improved accuracy compared to the matched non-fused and all non-fused groups for the striatum to occipital group (p=0.04, p=0.03), while the striatum to cerebellum ratio had improvement over the non-fused all group (p=0.041). MR fusion to FDOPA PET improves the accuracy of at least some measures (Striatum/Occiput, Striatum/Cerebellum) in the diagnosis of PD.

Keywords: 18F-Fluorodopa, positron emission tomography, image fusion, receiver operator characteristics, Parkinson's disease

Introduction

18F-Fluorodopa (FDOPA) is a radio-fluorinated dopamine precursor used in positron emission tomography (PET) imaging of the distribution of levodopa uptake. FDOPA is shown to accurately reflect the dopaminergic disturbances in Parkinson's disease (PD). [1-3] FDOPA PET uptake also correlates with PD symptom severity. [4, 5] Several quantitative methods are used in the interpretation of FDOPA PET data. The most commonly used tools are ratios of the time-averaged (static) signal in regions of interest (ROI) after equilibration of the radiotracer and graphical approaches to derive influx rate constants. [6] The graphical approach has the drawback of requiring dynamic scans of multiple time frames. The ratio methods use static scans similar in duration and procedure to clinical FDG-PET. The ratios measured (signal in striatum divided by that in a cerebellar or occipital cortex reference region) have shown diagnostic accuracy similar to the graphical approaches. [7, 8] A difficulty of the ratio methods is to accurately define the relevant anatomic structures particularly because the PET signal is often altered as part of the disease process. For example, FDOPA uptake in the striatum is altered in Parkinson's disease. In this disease, loss of nigrostriatal dopaminergic projections results in loss of PET signal in the posterior putamen. The posterior putamen can then be neglected in the striatal ROIs defined by PET signal.

Several techniques have been employed for locating the relevant structures (caudate, puta-

men) on the FDOPA PET. A common approach for research studies is to use institution-specific predefined ROIs, and then normalize the experimental images to these templates. [9-12] This technique requires institutional expertise not readily available to all centers that clinically use FDOPA PET. Another technique for ROI definition is to manually draw ROIs directly on the PET image based on radiologic experience. [13] This method is highly user dependent and can underestimate the anatomic extent of an area, especially the posterior putamen, due to loss of striatonigral projections and thus FDOPA uptake. Manually placing ROIs of fixed size has been suggested as a means to overcome this inherent problem. [8] However, fixed ROIs fail to account for inter-patient anatomic variability and age-related volume loss. Manually drawn ROIs may better account for this variability but are subject to high inter-reader variability, particularly when anatomic boundaries are indistinct.

One way to overcome the indistinct anatomic boundaries inherent to FDOPA PET is with fusion of the PET image to a magnetic resonance (MR) image. The PET image is co-registered to the MR by aligning 3-D renderings of the images sets. The fusion image then shows the PET as an overlay on the underlying MR images. In Parkinson's disease, T1 weighted MR image has greater contrast for defining subcortical grey matter structures such as the basal ganglia than does FDOPA PET. The improved localization of anatomic boundaries should theoretically allow for more accurate ROIs. We hypothesize that the improved localization of anatomic boundaries will allow for more accurate ROIs, and subsequently better diagnostic performance of FDOPA PET. Here we compare receiver operator characteristics (ROC) curves of FDOPA PET ratios: striatum-to-cerebellum, striatum-to-occipital cortex, anterior-to-posterior putamen, and caudate-to-post putamen generated with and without MR fusion. Receiver operator curves are a statistical method of comparing diagnostic tests with flexible cut-off points such as ratios.

**Materials and methods**

Subjects

Institutional Review Board approval was obtained for a retrospective analysis of PET images, the re-processing of images, and interrogation of clinical records for patients who have had clinical FDOPA scans at our institution (University of Wisconsin Hospital and Clinics) between 2000 and 2008. Inclusion criteria for this study included brain FDOPA PET for the diagnosis of Parkinson's disease (PD), at least 1 year of follow-up after PET scan, and a definitive diagnosis of PD or not PD by a movement disorder specialist. Exclusion criteria included having a movement disorder without diagnosis, less than one year of neurologic follow-up, and FDOPA PET for indication other than Parkinson-like syndrome (e.g. malignancy recurrence). After inclusion into the study, clinical and demographic factors at the time of the FDOPA PET were recorded. Standardized data from the electronic medical record were recorded (age at scan, sex); while other data was taken from clinic notes (lateralized physical exam findings, bradykinesia, rigidity, gait abnormality, cognitive/behavioral disturbance, and MRI available for fusion). Post-scan clinical records were examined for length of follow-up, age at diagnosis, and ultimate diagnosis.

Procedures and techniques

FDOPA Imaging: The FDOPA PET data used in this analysis were obtained using standard clinical scan procedures: Levodopa and other anti-Parkinson medications were held for 24 hours. Patients were premedicated with 200 mg of Carbidopa PO 1 hour prior to injection of 5-10 mCi of ¹⁸F-DOPA. The patient rested with minimal movement in a calm environment for the uptake period. Imaging started 110 minutes post injection. The patients were positioned supine in a scanner with help of cushioned a head holder. The PET images were obtained using a GE Advance PET scanner (General Electric Medical Systems, Waukesha, WI) starting with a 20 min 2D static acquisition, then a 5 min 3D static acquisition, followed by a 10 min transmission image. Images were reconstructed with iterative OSEM algorithms. T1 weighted, pre-contrast MR images were used for fusion. The MR that was most proximate to the FDOPA scan was used for fusion. Median length between MR and FDOPA PET was 1 yr with range 1 month to 5 years.

MRI Fusion: T1-weight MR images were fused with 2D attenuation corrected FDOPA PET images using commercially available software,
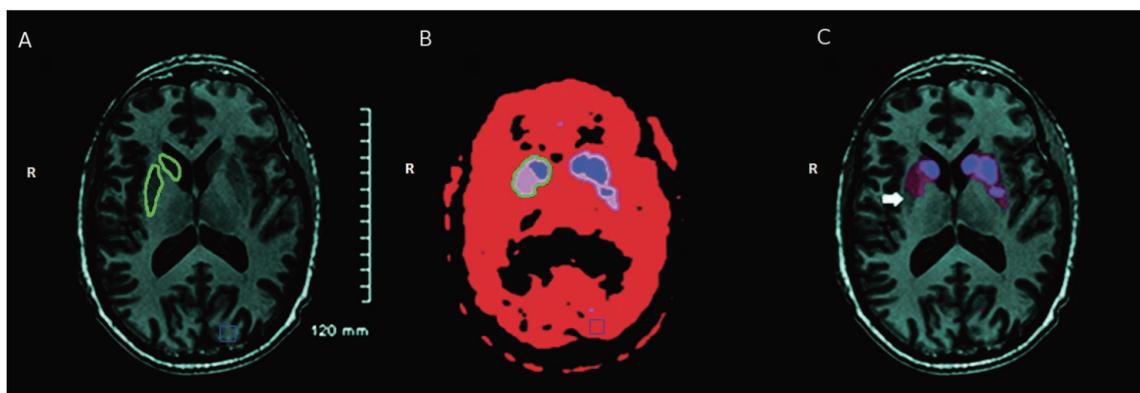
Figure 1. This is the T1 weighted MRI (A), FDOPA PET (B), and fused MRI/PET (C) of a patient with PD with left sided predominant symptoms. The right striatal ROIs are demarcated by a green line on the MRI and PET images. The blue lines demarcate the occipital lobe ROIs. The white arrow marks the area of the right posterior putamen that is incorporated into the MRI based ROI, but not the PET-based ROI. ROIs based solely on the FDOPA PET image can fail to accurately incorporate the entire anatomical reference. The right side of each image is marked with an R.

Advanced Fusion 7D (Build FUMK 1.0.0.10) © Siemens Medical Solutions USA, inc. The automatic affine deformable fusion algorithm was applied, and then the fusion was manually checked and adjusted. **Figure 1** is an example of the rendered fusion images. It shows a T1-weighted MRI, FDOPA PET, and the fused images of a patient with PD who at the time of imaging had predominantly left-sided symptoms. While the left striatum shows close anatomic and functional correlation between the PET and MRI, the right (pathologic side) of the striatum shows reduced FDOPA uptake in the posterior putamen that is not elevated above background. This area was part of the MRI ROI, but not the non-fused ROI.

ROIs: A rater blinded to the subject diagnosis drew four ROIs on each non-fused (NF) PET image series with only the PET data available. The order of studies was random. The rater then drew the ROIs on each MRI/PET fused series. The ROIs were right striatum, left striatum, cerebellum, and occipital cortex. The axial slice that bisects both caudate heads and has the largest anterior-posterior dimension of the striatum was used to draw all striatal ROIs on PET and MR. In most cases, this slice fell superior to the anterior commissure at the level of the columns of the fornix. To generate the occipital reference standard a square ROI of 100 mm^2 (10 mm x 10 mm) at the level that the striatal ROIs overlying the occipital cortex was used on both the PET and MRI. On MR scans the striatum was manually outlined at the gray/ white matter junction using Damasio's Human Brain Anatomy in Computerized Images as a visual reference. [14] The PET-based striatal ROIs were defined using a technique clinically developed at our institution. The striatum's approximate anatomic location was indentified based on gross anatomic landmarks, and then the specific ROIs borders were defined by being >10% (10% of maximum voxel) above the nearby insular cortex (estimated location). This border was clearly identifiable because the Mirada software allows a color change at 10% intervals of the maximum voxel.

For both PET and MR cerebellar ROI was defined at the level of the superior cerebellar peduncle. The PET anatomic boundary was defined by being > 10% above the cerebrospinal fluid (CSF) in peri-cerebellar subarachnoid space, and the boundary was the gray matter-CSF junction for the MR ROI. Both lateral hemispheres and the vermis of cerebellum were included for both PET and MR ROIs. The standard uptake value mean (SUVmean) was defined as the mean of the concentration of tracer for each voxel within an ROI divided by the injected dose over the body weight.

Statistical tests

The demographic and clinical data were compared between patients that had PD and did not have PD. Differences in characteristics between the PD and non-PD patients were assessed using Fisher's exact test for categorical data, and Mann-Whitney-Wilcoxon U test for

Table 1. Demographics of subjects

	Non-Parkinson's Disease	Parkinson's Disease	p-value
	Median (range)	Median (range)	Wilcoxon
Age at Diagnosis (years)	45 (41-61)	47.5 (29-76)	0.934
Age at PET Scan (years)	47 (43-67)	50 (33-78)	0.821
Clinical Follow-up (years)	4 (2-8)	5 (3-9)	0.197
	Proportion with (%)	Proportion with (%)	Fisher's Test
Sex (%male)	3/7 (42.9%)	15/20 (75.0%)	0.175
Lateralized findings	6/7 (85.7%)	15/19 (78.9%)	1.000
Bradykinesia	5/7 (71.4%)	11/18 (61.1%)	1.000
Tremor	4/7 (57.1%)	20/20 (100%)	0.012
Gait Disorder	4/6 (66.7%)	4/20 (20.0%)	0.051
Rigidity	3/7 (42.9%)	13/19 (68.4%)	0.369
Behavioral and/or Cognitive defect	3/5 (60.0%)	8/20 (40.0%)	0.623
MRI for fusion	5/7 (71.4%)	12/20 (60.0%)	0.678

*P-values <0.05 are in Bold; Dx; diagnosis.

continuous data. These statistical tests were carried out using JMP 9.0 Copyright © 2010, SAS Institute Inc., Cary, NC, USA.

The ROI derived SUVmean data were divided into three groups. That from the fused images (n=17), that from matched NF images (n=17), and that from all NF images (n=27). The total number of subjects was 27. 17 subjects had an available MRI for fusion. 10 subjects did not have an MRI available. The fused and matched NF data was derived from subjects who did have an MR for fusion, allowing for a direct comparison between fused and non-fused images. The "all non-fused" group consisted of data from both the matched NF images and subjects that did and did not have an MR for fusion. The striatum to cerebellum ratio (SCR) and striatum to occipital ratio (SOR) were calculated for each image set using the following formula:

Striatum (SUVmean)/Reference (SUVmean)

The reference SUVmean was defined as the mean SUV of either the cerebellum or occipital cortex for the respective ratio. This ratio was calculated for both the left striatum and right striatum. The lower of the ratios between the right and left was used for further analysis to account for asymmetric presentation of PD and corresponding asymmetry within the striatum. [15, 16] Within each of the three groups and for each ratio measure, the ideal cut-off point for the Striatum/Reference ratios was determined maximizing sensitivity and specificity [the highest geometric mean of sensitivity and specifici-

ty]. The sensitivity, specificity, positive predictive value (PPV), and negative predictive value were then calculated and reported with 95% confidence intervals by the method described by Agresti *et al*. [17] Given that sensitivity and specificity are subject to cut point biases, Receiver Operator Characteristics (ROC) curves with area under the curves (AUCs) were calculated. The ROC is a graph with the true positive rate on the Y-axis and the false positive rate on the X-axis. Because the sensitivity and specificity of a diagnostic test using a continuous variable (SCR, SOR) are a function of the point where the positive negative line is demarcating the ROC with the AUC provides a variable for uniform comparison between tests [18].

ROC analysis was carried out with the ROC-KIT GUI 1.0.3 © 2011 Chicago, IL. [19] The curve fits were estimated with non-parametric Wilcoxon and uncertainty was estimated with a bootstrapping technique. [20] AUCs are reported with two-sided 95% confidence intervals. The AUCs were compared with paired or partially paired significance tests described by Metz *et al*. [19] For all statistical tests the alpha level was set at 0.05.

Results

Demographic and clinical data

27 subjects met the inclusion /exclusion criteria. Of these subjects 7 had a diagnosis other than PD. These included somatization disorder (1 subject), anxiety/depression (1 subject), essential tremor disorder (1), corticobasal

Table 2. Imaging parameters characteristics

		AUC	Ideal Cut-Point	Sensitivity	Specificity
SOR	Fused	0.97 (0.88-1.00)	2.40	0.83 (0.54-0.96)	1.00 (0.51-1.00)
	Matched NF	0.63 (0.31-0.96)	3.00	1.00 (0.71-1.00)	0.40 (0.12-0.77)
	All NF	0.73 (0.48-0.97)	3.00	0.88 (0.74-1.00)	0.57 (0.25-0.84)
SCR	Fused	1.00 (1.00-1.00)	2.50	1.00 (0.71-1.00)	1.00 (0.51-1.00)
	Matched NF	0.82 (0.57-1.00)	2.50	1.00 (0.71-1.00)	0.60 (0.23-0.88)
	All NF	0.83 (0.65-1.00)	2.70	0.95 (0.74-1.00)	0.71 (0.35-0.92)

*For AUC equal to 1 the SE equal 0 hence the confidence interval has no range; AUC, area under curve; NF, not fused; SOR, striatum to occipital cortex ratio; SCR, striatum to cerebellum ratio.

degeneration (1 subject), hemi-dystonia (1 subject), psychiatric disorder not otherwise specified (1 subject), and non-PD degenerative neurologic disorder (1). Each subject had at least 2 years of clinical follow-up after PET. **Table 1** is a summary and comparison of the patients whose scans were included in the study. The only significant difference in clinical findings described in the "physical examination" section of clinic documents between the PD and Non-PD patients was tremor. All of the PD (20/20) had a tremor while only 4/7 of non-PD patients did. Ten patients did not have a fusible MR; seven of these subjects did not have an MR at the institutional picture archiving and communication system (PACS) while 3 subjects MR were in a format not usable to the fusion software. These MR images were digital copies of filmed MR images from outside institutions.

ROC analysis

For both fused and NF FDOPA ROI data, the ratios (SOR, SCR) were calculated. ROC curves were then generated for each ratio for three sets of data, FDOPA fusion (n=17), matched NF FDOPA (n=17), and NF FDOPA for all subjects (n=27). For each ratio the AUC, the ideal cut-off point ratio, and sensitivity/specificity at that ideal cut-off point are summarized in **Table 2**. The fused image group had the highest AUC (95% CI) for each of the measures: SOR [0.97 (0.88-1.00)] and SCR [1.00 (1.00-1.00)]. It should be noted that for an AUC of one the standard error equals zero, and the confidence interval has no range. This does not imply that AUC is 1 with complete certainty, but is a function of the statistical formula. [19] The matched NF had the lowest AUCs: SOR [0.63 (0.31-0.96)] and SCR [0.82 (0.57-1.00)]. The AUCs were improved with the addition of more subjects in the All NF groups: SOR [0.73 (0.48-0.97)] and

SCR [0.83 (0.65-1.00)]. The confidence intervals overlapped between the various ratio measures and between the imaging groups, but further testing was used to determine if a difference is present. [21]

Comparison of AUCs

The AUC's were compared between ROI data sets (fused, all NF, and matched NF) **Table 3** lists these results. The AUC was significantly higher for fused data compared to matched NF group for the SOR (p=0.040), and the to the all NF group for the SOR (p=0.030) and SCR (p=0.041). There was also a trend (P<0.10) toward statistical significance in the SCR for fused versus matched NF (p=0.067), and in both fused versus matched NF (p=0.084), and versus all NF (p=0.060). No other comparisons were statistical different. Between the SOR, SCR neither ratio was shown to have a significantly higher AUC. This was true in the fused group, the NF matched, and the NF all.

Discussion

The primary result of this study is that MR fusion increases the AUC and the predictive accuracy for the SOR and SCR of FDOPA PET. The comparisons between fused and NF images for SOR were statistically significant. For the SCR the all NF group was statistically significant and the NF matched showed a trend toward statistical significance. Comparison between the SOR and the SCR did not show any significant differences. The SCR did have uniformly higher AUCs than the SOR for the fused and NF groups. The cerebellum may have performed as a more stable reference standard because the ROI used for the cerebellum was much larger (both hemispheres and vermis) than the occipital reference standard (100 mm^2 at the level of the basal ganglia).

Table 3. AUC comparison

		Delta AUC	Z-score	p value
SOR	Fused v NF (Matched)	0.334	1.755	0.040
	Fused v NF (all)	0.238	1.876	0.030
SCR	Fused v NF (Matched)	0.183	1.500	0.067
	Fused v NF (all)	0.171	1.737	0.041
Fused FDOPA-PET	SOR v SCR	0.033	0.849	0.198
NF (Matched)	SOR v SCR	0.104	0.358	0.640
NF (All)	SOR v SCR	0.100	0.523	0.300

*Delta AUC, difference in AUCs; #p-values in bold are statistically significant (p<0.05), p-values in italics show a trend toward statistical significance (p<0.10); SOR, striatum to occipital cortex ratio; SCR, striatum to cerebellum ratio; NF, not fused.

It follows that MRI fusion may better predict pathology by improving the accuracy of ROI placement, and thus of ratios derived from these ROIs. The ROIs on the FDOPA PET (the non-fused images) used a set level above background cortex (10%), while the MR uses gray/white matter differentiation of the basal ganglia as ROI boundaries. The pathologic process of PD decreases this striatal FDOPA uptake in a posterior to anterior manner. [22] Thus, ROIs drawn directly on PET over-estimate residual activity (SUVmean) in the posterior putamen. The MRI has the advantage of allowing ROIs to be defined structurally rather than functionally.

Pan *et al.* recognized that posterior putamen signal loss was a potential confounder with FDOPA PET images and proposed that a fixed size of ROI should be maintained for the striatum. This method is superior to ROI defined by a percentage above background or within a maximum, but it fails to account for individual variations in brain structure. Even small amounts of cortex and white matter in an ROI intended to be part of the putamen could depress the SUVmean resulting in increased false positives, making the test less accurate for patients with cerebral volume loss. A study with similar methods (using MRI for ROI generation), but aimed at comparing the graphical and ratio methods, found AUCs similar to this study. With 89 subjects, AUCs of 0.99, 0.99, and 0.79 were found for the caudate, anterior putamen, and posterior putamen contralateral to predominant symptoms. [12] It is clear that FDOPA PET interpretation can be aided with simple adjunct quantitative measures such as mean SUV ratios from ROIs drawn with MR fusion. In this study the entire striatum was used for a region of interest, but dividing the striatum into several parts (as in the previously cited study) or even voxel-based analysis can allow for improved discriminatory power for disease states with more subtle pathophysiologic differences like multiple systems atrophy and PD, but proper function-anatomic correlation with techniques like MR/PET fusion is necessary for these techniques to reach their full potential. Long and complex post-image processing is not necessary for highly reliable and accurate results, but one has to be cautious in defining ROIs strictly based on percentages above background or on the voxel with the highest uptake.

This study only had 27 subjects, and of these only 17 had an MR that was fusible, but the study size was adequate to detect a difference between several measures, however this study has low power due to low sample size, and that the significant findings could be due to multiple testing, and are subject to further verification. More complex means of ROI creation including deformation into Montreal Neurologic Institute space with preformed ROIs might offer even greater inter-reader reliability and discriminatory power, but would retain problems with imperfect co-registration of subcortical structures between subjects. A study comparing these methods to manual per subject ROI drawing is yet to be completed, but these more advanced techniques do not seem necessary for accurate reliable clinical interpretation of FDOPA PET. The reference standard used for diagnosis in this study is the clinical follow-up by a movement disorder specialist. This is the current gold standard for diagnosis of premorbid Parkinson's disease. However, the specialist was not blinded to the results of the FDOPA PET and this is a potential area of bias. The patient's long follow-up (median 4 years) probably lessened this bias, as the influence of decreases over time and as the disease progresses, diagnosis become more evident.

A potential drawback of this technique is that not all patients have an MR available for fusion. Ten of the 27 patients in this study did not have a fusible MR. The main reasons for not having a fusible MR were that an MR was not available in PACS or that is was a scanned image of film MR. All of these patients had a head MR at some point in their clinical work-up, but generally this was done prior to referral to a specialist in movement disorders. These images were often sent with the patient in a film format or scanned film format, and not as a DICOM file. Within the last several years PACS systems have become a standard at even small health-care facilities. This should allow for greater accessibility and ease in fusing FDOPA PET and MR for referral centers, mitigating this problem in the future. It should be noted that for PET studies in general that do not have appropriate anatomic scan for fusion, SUVmax remains a valid measure that is less likely to be influenced by ROI placement.

This study demonstrates that MRI fusion with FDOPA PET via readily available commercial software improves at least some of the quantitative measures used to clinically interpret FDOPA PET. Nuclear medicine physicians and radiologists may want to explore MR fusion for FDOPA PET interpretation within their own software/hardware paradigm. FDOPA PET is another clinical scenario where PET/MRI may show an advantage in the future. Potentially MR fusion will also find a role in the recently FDA approved dopamine transport single photon emission tomography (SPECT).

Acknowledgements

Conflict of interest statement

None of the authors have financial or editorial conflicts of interest to claim.

Address correspondence to: Dr. Lance Hall, Box 3252 Clinical Science Center-E3 600 Highland Ave Madison, WI 53792. Telephone: (608) 263-5585; Fax: (608) 265-7390; E-mail: lhall@uwhealth.org

Reference

[1] Pate BD, Kawamata T, Yamada T, McGeer EG, Hewitt KA, Snow BJ, Ruth TJ and Calne DB. Correlation of striatal fluorodopa uptake in the MPTP monkey with dopaminergic indices. Ann Neurol 1993; 34: 331-338.

[2] Snow BJ, Tooyama I, McGeer EG, Yamada T, Calne DB, Takahashi H and Kimura H. Human positron emission tomographic [¹⁸F] fluorodopa studies correlate with dopamine cell counts and levels. Ann Neurol 1993; 34: 324-330.

[3] Pavese N, Rivero-Bosch M, Lewis SJ, Whone AL and Brooks DJ. Progression of monoaminergic dysfunction in Parkinson's disease: A longitudinal (¹⁸F)-dopa PET study. Neuroimage 2011; 56: 1463-1468.

[4] Antonini A, Vontobel P, Psylla M, Gunther I, Maguire PR, Missimer J and Leenders KL. Complementary positron emission tomographic studies of the striatal dopaminergic system in Parkinson's disease. Arch Neurol 1995; 52: 1183-1190.

[5] Pal PK, Lee CS, Samii A, Schulzer M, Stoessl AJ, Mak EK, Wudel J, Dobko T and Tsui JK. Alternating two finger tapping with contralateral activation is an objective measure of clinical severity in Parkinson's disease and correlates with PET. Parkinsonism Relat Disord 2001; 7: 305-309.

[6] Hoshi H, Kuwabara H, Leger G, Cumming P, Guttman M and Gjedde A. 6-[¹⁸F]fluoro-L-dopa metabolism in living human brain: a comparison of six analytical methods. J Cereb Blood Flow Metab 1993; 13: 57-69.

[7] Dhawan V, Ma Y, Pillai V, Spetsieris P, Chaly T, Belakhlef A, Margouleff C and Eidelberg D. Comparative analysis of striatal FDOPA uptake in Parkinson's disease: ratio method versus graphical approach. J Nucl Med 2002; 43: 1324-1330.

[8] Pan XB, Wright TG, Leong FJ, McLaughlin RA, Declerck JM and Silverman DH. Improving influx constant and ratio estimation in FDOPA brain PET analysis for Parkinson's disease. J Nucl Med 2005; 46: 1737-1744.

[9] Moore RY, Whone AL and Brooks DJ. Extrastriatal monoamine neuron function in Parkinson's disease: an ¹⁸F-dopa PET study. Neurobiol Dis 2008; 29: 381-390.

[10] Pavese N, Moore RY, Scherfler C, Khan NL, Hotton G, Quinn NP, Bhatia KP, Wood NW, Brooks DJ, Lees AJ and Piccini P. In vivo assessment of brain monoamine systems in parkin gene carriers: a PET study. Exp Neurol 2010; 222: 120-124.

[11] Tzourio-Mazoyer N, Landeau B, Papathanassiou D, Crivello F, Etard O, Delcroix N, Mazoyer B and Joliot M. Automated anatomical labeling of activations in SPM using a macroscopic anatomical parcellation of the MNI MRI single-subject brain. Neuroimage 2002; 15: 273-289.

[12] Jokinen P, Helenius H, Rauhala E, Bruck A, Eskola O and Rinne JO. Simple ratio analysis of ^{18}F-fluorodopa uptake in striatal subregions separates patients with early Parkinson disease from healthy controls. J Nucl Med 2009; 50: 893-899.

[13] Brown WD, Taylor MD, Roberts AD, Oakes TR, Schueller MJ, Holden JE, Malischke LM, DeJesus OT and Nickles RJ. FluoroDOPA PET shows the nondopaminergic as well as dopaminergic destinations of levodopa. Neurology 1999; 53: 1212-1218.

[14] Damasio H. Human Brain Anatomy in Computerized Images. New York: Oxford University Press, 1995.

[15] Leenders KL, Palmer AJ, Quinn N, Clark JC, Firnau G, Garnett ES, Nahmias C, Jones T and Marsden CD. Brain dopamine metabolism in patients with Parkinson's disease measured with positron emission tomography. J Neurol Neurosurg Psychiatry 1986; 49: 853-860.

[16] Nahmias C, Garnett ES, Firnau G and Lang A. Striatal dopamine distribution in parkinsonian patients during life. J Neurol Sci 1985; 69: 223-230.

[17] Agresti A and Coull BA. Approximate Is Better than "Exact" for Interval Estimation of Binomial Proportions. The American Statistician 1998; 52: 119-126.

[18] Zou KH, O'Malley AJ and Mauri L. Receiver-operating characteristic analysis for evaluating diagnostic tests and predictive models. Circulation 2007; 115: 654-657.

[19] Metz CE, Herman BA and Roe CA. Statistical comparison of two ROC-curve estimates obtained from partially-paired datasets. Med Decis Making 1998; 18: 110-121.

[20] Mossman D. Resampling techniques in the analysis of non-binormal ROC data. Med Decis Making 1995; 15: 358-366.

[21] Wolfe R and Hanley J. If we're so different, why do we keep overlapping? When 1 plus 1 doesn't make 2. CMAJ 2002; 166: 65-66.

[22] Nurmi E, Ruottinen HM, Bergman J, Haaparanta M, Solin O, Sonninen P and Rinne JO. Rate of progression in Parkinson's disease: a 6-[^{18}F]fluoro-L-dopa PET study. Mov Disord 2001; 16: 608-615.